Los Alamos
NATIONAL LABORATORY
EST. 1943

LA-UR-21-25649
Approved for public release; distribution is unlimited.

Title: Spot Size Optimization of the Scorpius Accelerator

Author(s): Burris-Mog, Trevor John

Intended for: Report

Issued: 2021-06-15

Disclaimer:
Los Alamos National Laboratory, an affirmative action/equal opportunity employer, is operated by Triad National Security, LLC for the National Nuclear Security Administration of U.S. Department of Energy under contract 89233218CNA000001. By approving this article, the publisher recognizes that the U.S. Government retains nonexclusive, royalty-free license to publish or reproduce the published form of this contribution, or to allow others to do so, for U.S. Government purposes. Los Alamos National Laboratory requests that the publisher identify this article as work performed under the auspices of the U.S. Department of Energy. Los Alamos National Laboratory strongly supports academic freedom and a researcher's right to publish; as an institution, however, the Laboratory does not endorse the viewpoint of a publication or guarantee its technical correctness.

Spot Size Optimization of the Scorpius Accelerator

Trevor J. Burris-Mog

ASD Scorpius Project

April 2021

Introduction

The Scorpius Linear Induction Accelerator (LIA) is being developed by the Advanced Sources and Diagnostics (ASD) Project and will complement other U1a capabilities by providing a multi-pulse, DARHT-class, flash-radiography capability. Commissioning activities are expected to end in Spring of 2026. All of the diagnostics discussed in this chapter are relevant to LIAs that generate high-current relativistic electron beams, and some diagnostics will also be relevant to other accelerators.

The Scorpius Accelerator will be the world's most advance LIA. Although significant technological advancements have been incorporated throughout the machine, many performance aspects of Scorpius will be similar to those of FXR and DARHT Axis-I and -II. These LIAs offer the same challenges, whether it is suppressing beam instabilities, improving diagnostic accuracy, validating computer simulations and beam tunes, or reducing beam-target interaction effects. However, the ultimate figure of merit is consistent between these LIAs, which is spot size and dose.

Beam Parameters of Interest

With enough knowledge of the beam parameters, an LIA's systems can be optimized. The beam parameters under some degree of control[1] are the beam energy spread ($\Delta\gamma$), radius (R_0), convergence (R_0/z), normalized Lapostolle [4 rms] emittance (ϵ_n) and beam motion. The amount of influence that each beam parameter has on the spot size is found by taking the quadrature sum of the contributing terms: $r_{spot}^2 = (\frac{\epsilon_n z}{\beta\gamma R_0})^2 + (2R_0\frac{\Delta\gamma}{\gamma})^2 + (C_s R_0^3)^2$. Figure 1 shows how these parameters scale with respect to the beam radius (R_0) at the entrance of the final focus solenoid for the nominal beam parameters of $C_s = 0.0027132$ cm^2, $\delta\gamma/\gamma = 2\%$ and $\epsilon = 1000$ mm-mrad. The beam motion and beam-target interactions scaling is presented as a fractional increase of the quadrature sum, since each grow the integrated spot size.

The table shown in Figure 2 presents the nominal values and allowable variations for the beam current, energy and emittance on Scorpius, as well as measured values and uncertainties for radius, convergence, emittance and energy from either Axis-I or -II. Understanding the present limitations along with how the parameters scale the spot size allows us to prioritize our efforts. For example, the measurement uncertainty for beam emittance has more room for improvement than that of the beam energy.

[1]Beam current (i.e. charge Q on target) and beam energy (E) are fixed by dose requirements. In very simplified terms, the dose (D) scales approximately as $D \propto QE^{2.8}$.

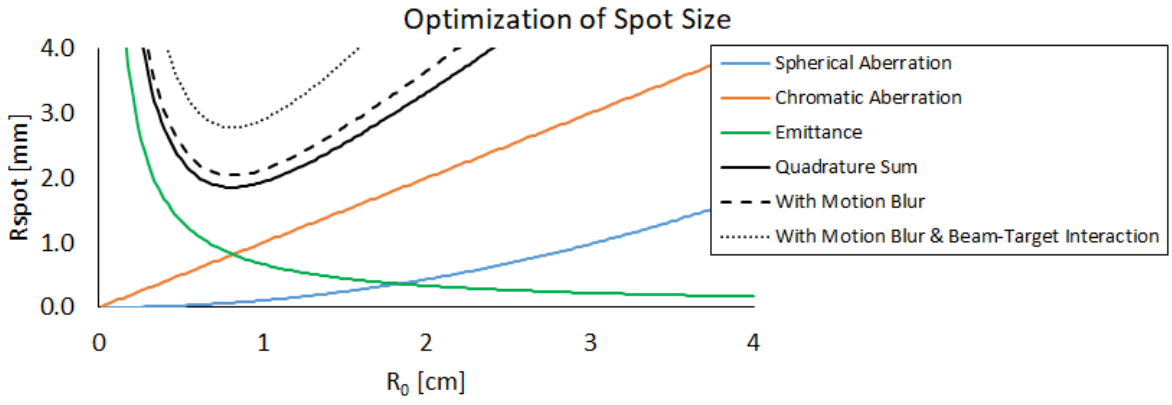

Figure 1: This image shows how the beam parameters influence the spot size: Spherical Aberration $C_s = 0.0027132$ cm^2, Energy Spread $\delta\gamma/\gamma = 2\%$, Emittance $\epsilon = 1000$ mm-mrad, with motion blur and beam-target interactions increasing the integrated spot size by 10% and 50% respectively.

Accurate measurements of beam parameters are also vital inputs into the beam transport codes used to develop optimum tunes. Figure 3 shows the envelope radius of a 200 mm-mrad beam as transported with an optimized tune. A 400 mm-mrad beam transported in the same tune results in poor transport and a doubling of the spot size. Accurate beam measurements are required to optimize an accelerator.

Beam Target Interactions

Beam-target interactions are thought to increase the integrated spot size by 40% to 80% on Axis-II and almost double on Axis-I, making them a priority to understand and mitigate. Beam-target interactions come in two forms, and both are driven by Ohmic heating of the bremsstrahlung converter target.

The first form of beam-target interaction occurs when the high-current electron beam heats the target, which leads to thermal desorption of surface contaminants. Thermal desorption[2] begins around 400° C, which is reached within the first few nanoseconds of the

[2]The desorbed flux $dn/dt = -vn(t)d^{-Q/RT}$, where $v \approx 10^{13}$ s^{-1} is the desorption rate, n is the amount of surface contaminants [atoms cm^{-2}] and the ratio of binding energy to target temperature is in the exponent.

Parameter	Measurement Location	Allowable Variation	Nominal Values
Beam Current	Exit of Injector	<1% RMS	2 kA ± 28 A
Beam Energy	Exit of Injector	<1% RMS	2 MeV ± 28 keV
Beam Energy	In Accelerator	<5% RMS	Location dependent
Beam Energy	Exit of Accelerator	<2% RMS	20 MeV ± 566 keV
Beam Energy	Entrance to Final Focus Solenoid	<1% RMS	20 MeV ± 283 keV
Beam Emittance	Exit of Accelerator	N/A	<1000 mm-mrad

Parameter	Measurement Location	Measured Values	Present Measurement Uncertainty
Beam Radius	Exit of Axis-II	1.59 cm	0.13 cm
Beam Convergence	Exit of Axis-II	3.10 cm	0.56 cm
Beam Emittance	Exit of Axis-II	700 mm-mrad	220 mm-mrad
Beam Energy	Exit of Axis-I	19.85 MeV	64 keV

Figure 2: **Top** - Allowable variations for the Scorpius accelerator. **Bottom** - Uncertainties for measurements performed on Axis-I and -II.

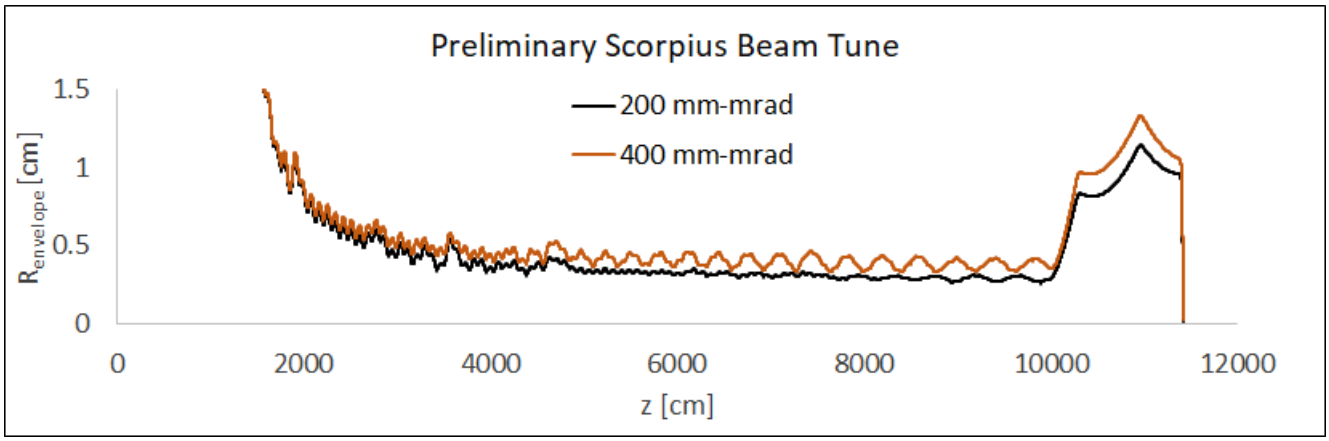

Figure 3: Output from the XTR envelope code showing the envelope radius of a 200 mm-mrad beam as transported with an optimized tune. A 400 mm-mrad beam transported in the same tune results in poor transport and a doubling of the spot size.

beam-target interaction. The desorbed species are quickly ionized by the electron beam and move upstream due to the electron beam potential well. Space charge limited emission from the target is reached and the upstream moving ions neutralize[3] the electron beam. The result is a dynamic "flying" focus [1, 2, 3, 4] as seen in the measured data presented in Figure 4. Thermal desorption affects both single and multi-pulse LIAs and attempts to mitigate this effect have been made [5, 6] and proposed [7].

[3] $K = \frac{2I}{\beta^3 \gamma I_0}\left[\frac{1}{\gamma^2} - f\right]$, where I_0 = -17,000 [A] and f is the fraction of any neutralizing (positive) species that can alter the focus.

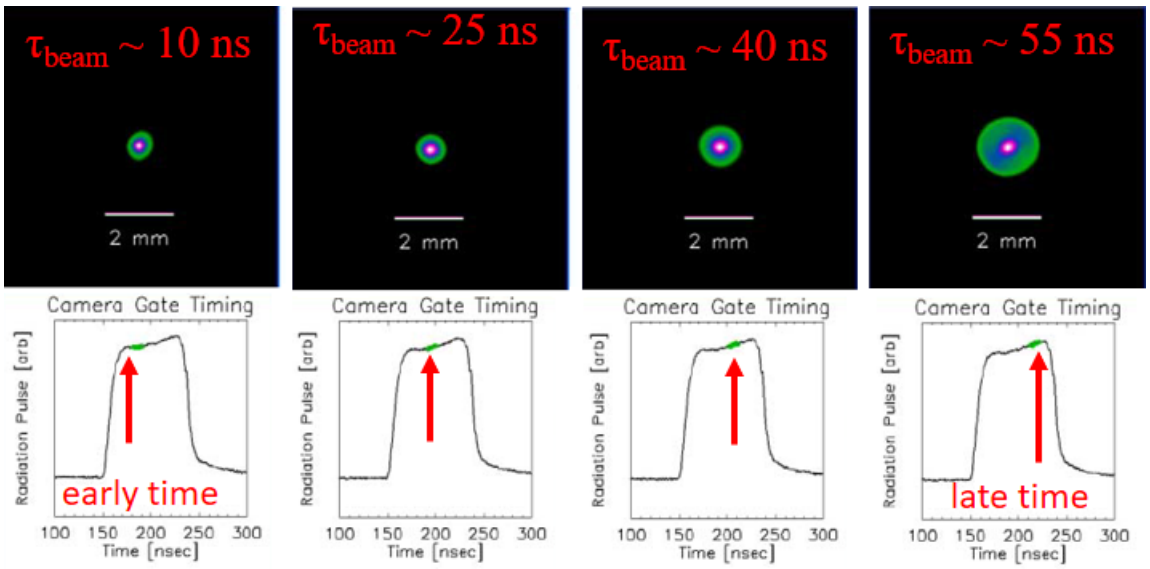

Figure 4: Images from the Time Resolved Spot Size (TRSS) diagnostic capturing the dynamic focus on DARHT Axis-I [1]

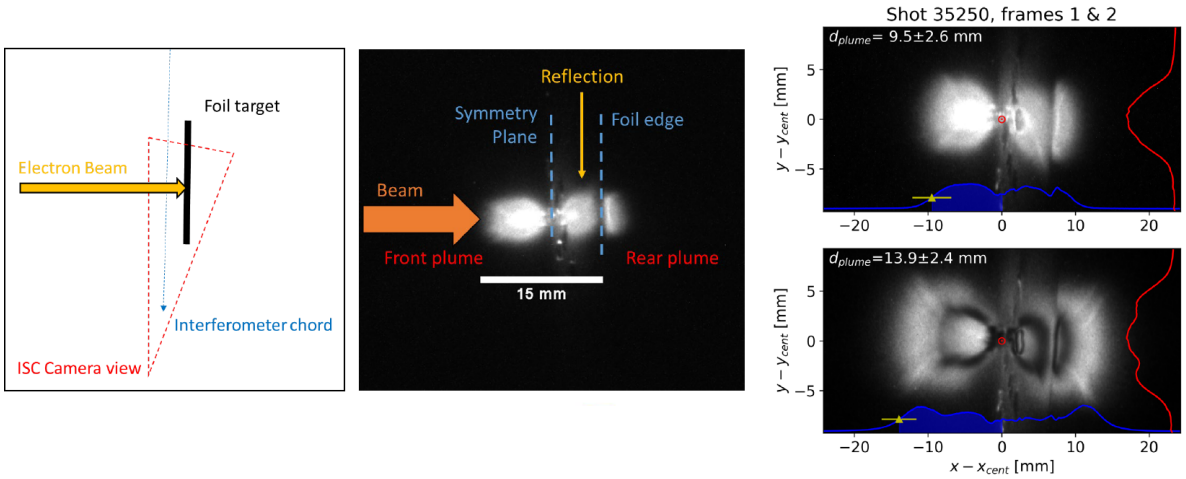

Figure 5: Images of a thin foil target expansion after interaction with the Axis-II electron beam.

The second form of beam-target interaction occurs when the target material is heated to the vapor and plasma phases, which is relevant to multi-pulse LIAs but not necessarily single-pulse LIAs. Figure 5 shows an image of the target expansion after the DARHT Axis-II electron beam interacts with a thin-foil target[4]. As the target expands, its density is reduced and ultimately beam-plasma interactions occur. The need for higher doses at later pulses further increases the per pulse heating of the target.

Diagnostic Challenges

The ASD Project is developing beam diagnostics with support from its partner institutions[5], and Figure 6 list these diagnostics along with the beam parameters they measure. It's important to consider the many limitations that exist when designing and fielding diagnostics on an LIA and that diagnostics can be surprisingly invasive. An example of an invasive diagnostic is a thin (ten's of microns) foil used to image the electron beam via optical transition radiation and/or Cherenkov radiation. The scatter through such a foil may be negligible, however the foil shorts the beam's electric field causing the beam to focus itself, altering the beam transport downstream of the diagnostic.

Another area to be cautious around is heating a diagnostic that is placed inside the

[4]Images provided by Michael Jaworski, Kimberly Schultz, Martin Schulze.
[5]LANL, LLNL, NNSS and SNL

beam. Of course significant heating can damage the diagnostic altogether and may even lead to contaminating accelerator cell gaps with the debris. But heating doesn't have to destroy the diagnostic in order to influence the measurement. Thermal desorption of surface contaminants begins around 400° C. The desorbed species are quickly ionized by the relativistic electron beam and begin to move upstream due to the electron beam's potential well. This leads to a dynamic focusing of the beam due to the neutralization of the beam's electric field, altering the beam transport upstream of the diagnostic.

Something else to consider is that not all diagnostics need to be placed in the beam's path to be invasive. Diagnostic stations and pump crosses have built in conducting rods and meshes to keep return current symmetry in areas where there are gaps. This is to avoid the buildup of detrimental wakefields than can destroy the electron beam. Placing a diagnostic

Diagnostic	Beam Parameter	Additional Information		
Beam Position Monitors	Current, Centroid	Permanent Diagnostic	Non-Invasive	Time Resolved
Fast Beam Positioning Monitors	Current, Centroid	Permanent Diagnostics	Non-Invasive	Time Resolved
Voltage Monitors	Energy	Permanent Diagnostic	Non-Invasive	Time Resolved
Titanium Foil & PiMax	Beam Profile	Temporary Diagnostic	Invasive	Time Integrated
Titanium Foil, PiMax & Solenoid Scan	Emittance	Temporary Diagnostic	Invasive	Time Integrated
Anamorphic Streak Imaging	Beam Profile	Temporary Diagnostic	Invasive	Time Resolved
Electron Spectrometer & Streak Camera	Absolute Energy	Temporary Diagnostic	Invasive	Time Resolved
Diamagnetic Loop	Radius, Convergence	Permanent Diagnostic	Quasi Non-Invasive	Time Resolved
Radiographic Camera	Resolution & Signal	Permanent Diagnostics	Non-Invasive	Time Integrated

Figure 6: Conventional diagnostics being developed by the ASD Project for the Scorpius Accelerator.

inside the radius of the beam pipe can generate detrimental wakefields that steer the beam. Therefore, a diagnostic doesn't need to "touch" the beam in order to affect the beam.

Measuring beam-target interactions also has its own set of challenges. For one, the target becomes a bright source of mostly forward directed bremsstrahlung and 4-π emitted neutrons, which may affect certain diagnostics. Other challenges are line-of-sight access to the target. Bulky shielding and the final focus solenoid greatly limit the visible access to the target. Most often, beam-target interactions are studied at a diagnostic station positioned downstream from a transport solenoid, however this limits the target thickness in order to reduce the risk of contaminating the accelerator cells with target debris.

Conversation

Beam measurements inform us of the accelerator's performance and provide input parameters to the computer codes used for beam transport and beam-target simulations. Ideally, all beam parameters would be measured with non-invasive diagnostics that have very low

Conserved Quantity	Plume/Plasma	Diagnostic Technique	Beam	Diagnostic Technique
Mass	Density	Two-Color Interferometer (TCI), Thomson Scattering (TS), Filtered Plume Imaging, Shadowgraphy	Current and Current Density	BPMs, Optical Transition Radiation, Pinhole imaging, Characteristic X-ray Emission
Momentum	Velocity	PDV (early time), Spectroscopy (e.g. Doppler shift), Thomson Parabola, Multi-frame Shadowgraph, Multi-chord TCI, Faraday Cup/Charge Collectors	Transverse emittance	Pepperpot, Optical Transition Radiation with solenoid scan (near/far)
Energy	Ion Energy, Temperature	Thomson Parabola, Thomson Scattering, Spectroscopy (e.g. line ratios)	Longitudinal Energy Spread	Magnet Spectrometer, Compton Spectrometer

Figure 7: Diagnostics being developed or considered for DARHT beam-target interaction studies. Filtered plume imaging and x-ray shadowgraphy are being developed in a collaboration between LANL and the NNSS.

uncertainties. However, as shown in Figure 6, a number of diagnostics are invasive and cannot be used during a hydrodynamic or subcritical experiment, which is good motivation to advance our diagnostic technology.

One example of how we are advancing diagnostics is the diamagnetic loop. The invasive nature of using imaging foils to measure the beam's radius and convergence is the driving force behind the development of the diamagnetic loop, which has been demonstrated to non-invasively measure the beam radius and beam emittance by measuring the change in magnetic flux of a relativistic electron beam traveling through a solenoid's magnetic field [8, 9].

Advancing our non-invasive diagnostics to measure beam parameters is important, but our ultimate figure of merit is the spot size, which is determined by pinhole or rolled edge measurements. Because these measurements cannot be performed during hydrodynamic and subcritical experiments, they are made ahead of time an assumed to remain within a given shot-to-shot variation. A novel approach has been suggested that takes advantage of the x-rays (bremsstrahlung and/or characteristic) that emerges from the upstream side of the target, i.e. the rear side of the source used to create the radiograph [10]. Measuring the rear spot size can provide direct correlation of the spot size and the image resolution of the radiograph.

Concluding Remarks

As with any technology, making significant advancements can be difficult. Appropriate planning is always necessary to inform our decisions, and Figure 1 along with a list of measurement uncertainties can provide a quick guide to what our diagnostic priorities should be.

References

[1] B T McCuistian, H Bender, C Carlson, C G Hollabaugh, D C Moir, E A Rose, and R Trainham. Temporal Spot Size Evolution of the DARHT First Axis Radiographic Source. page 3 p, 2008.

[2] C. Vermare, H. A. Davis, D. C. Moir, and T. P. Hughes. Ion emission from solid surfaces induced by intense electron beam impact. *Physics of Plasmas*, 10(1):277–284, 2003.

[3] Dale R. Welch and Thomas P. Hughes. Effect of target-emitted ions on the focal spot of an intense electron beam. *Laser and Particle Beams*, 16(2):285–294, 1998.

[4] Jun Zhu, Nan Chen, Haijun Yu, Xiaoguo Jiang, Yuan Wang, Wenhua Dai, Feng Gao, Minhong Wang, Jin Li, and Jinshui Shi. Back-streaming ion emission and beam focusing on high power linear induction accelerator. *Physical Review Accelerators and Beams*, 14(8), 2011.

[5] M. E. Cuneo. The effect of electrode contamination, cleaning and conditioning on high-energy pulsed-power device performance. *IEEE Transactions on Dielectrics and Electrical Insulation*, 6(4):469–485, 1999.

[6] Yu-Jiuan Chen, James F. McCarrick, Gary Guethlein, George J. Caporaso, Frank Chambers, Steven Falabella, Eugene Lauer, Roger Richardson, Steve Sampayan, and John Weir. High Intensity Beam and X-Ray Converter Target Interactions and Mitigation. *AIP Conference Proceedings*, 647(1):240–254, 2002.

[7] T.J. Burris. Heated Bremsstrahlung Targets to Mitigate Spot Size Growth at DARHT. Technical report, 2018.

[8] C.A. Ekdahl. Non-Invasive Monitoring of Beam Parameters Using Diamagnetic Loops. Technical report, 1999.

[9] W.B. Broste and H.V. Smith. Diamagnetic Loop Status. Technical report, 2020.

[10] P. A. Kolesnikov, V. Yu. Politov, E. S. Li, A. P. Yaskevich, S. A. Kolesnikov, Yu. M. Ekimov, M. A. Malyshev, A. R. Akhmetov, D. V. Petrov, O. A. Nikitin, I. V. Penzin, Yu. A. Trunev, M. G. Atlukhanov, A. V. Burdakov, V. V. Danilov, V. V. Kurkuchekov, S. S. Popov, D. I. Skovorodin, and K. I. Zhivankov. Technique for measuring of LIA spot size on target by X-rays propagating in beam backward direction. *Journal of Instrumentation*, 15(10):P10018, October 2020.